






Neutron Star Bounds on Muonic Fifth Forces from Picometer to Kilometer Scales

Damiano F. G. Fiorillo ^{1,2} Alessandro Lella ^{3,4} Georg G. Raffelt ⁵
Nudžeim Selimović ^{3,4} and Edoardo Vitagliano ^{3,4}

¹*Istituto Nazionale di Fisica Nucleare (INFN), Sezione di Napoli,
Complesso Universitario di Monte Sant'Angelo, Via Cintia, 80126 Napoli, Italy*

²*Gran Sasso Science Institute (GSSI), L'Aquila, Italy*

³*Dipartimento di Fisica e Astronomia, Università degli Studi di Padova, Via Marzolo 8, 35131 Padova, Italy*

⁴*Istituto Nazionale di Fisica Nucleare (INFN), Sezione di Padova, Via Marzolo 8, 35131 Padova, Italy*

⁵*Max-Planck-Institut für Physik, Boltzmannstraße 8, 85748 Garching, Germany*

Experimental searches for fifth forces coupled to muons are fundamentally limited by the scarcity of muons in ordinary matter, whereas neutron stars contain abundant muon populations. We show that these compact objects therefore provide superior sensitivity across a broad range of mediator masses. Neutron-star cooling implies limits of $g_{\phi\mu} \lesssim 10^{-12}$ and $g_{V\mu} \lesssim 3 \times 10^{-13}$ on scalar and vector bosons with masses $m_X \lesssim 100$ keV, whereas SN 1987A cooling implies only $g \lesssim 3 \times 10^{-9}$. Moreover, hydrostatic equilibrium requires any long-range muonic force to be sufficiently weak, surpassing cooling bounds for $m_X \lesssim 10^{-5}$ eV. Together, these observables provide the most stringent probes of muonic interactions over distance scales ranging from picometers to kilometers.

Introduction—Novel forces beyond the four known fundamental interactions—gravitational, electromagnetic, strong, and weak—could arise from the existence of new light bosons. Although Casimir measurements [1, 2], microcantilevers [3], torsion-balance experiments [4–9], and satellite-borne accelerometers [10] provide powerful probes of fifth forces, they rely on ordinary matter and therefore have limited sensitivity to interactions that couple preferentially to muons.

Muonic bosons have been proposed as gauge bosons of a new $U(1)_{L_\mu-L_\tau}$ symmetry [11–14], but also in the form of new scalars [15, 16] or pseudoscalars (e.g. Ref. [17] and references therein), all phenomenologically described by a gauge or Yukawa coupling $g_{X\mu}$ and mass m_X , where $X = \phi, a, V$ (scalar, pseudoscalar and vector bosons). The quest for muonic fifth forces then amounts to the simple question: how strongly can such low-mass bosons couple to muons?

Remarkably, the most restrictive tests are obtained from neutron stars (NSs). Despite the large muon mass of $m_\mu = 105.7$ MeV, these compact astrophysical objects contain substantial muon populations thanks to beta equilibrium, making NSs unique laboratories for muonic interactions. In a reference model for a medium-aged NS (see End Matter), typical abundances are $Y_p \simeq 0.10$ for the average proton fraction per baryon, and $Y_e \simeq 0.06$ and $Y_\mu \simeq 0.04$. In previous works, the large muon densities of pulsars [18, 19] and proto-neutron stars [20–24] were used to constrain muonic fifth forces with very long and very short interaction range λ , corresponding to very small and very large boson mass, respectively.

In this Letter, we identify two new observables, probing large uncharted regions of the muonic boson parameter space, shown red in Fig. 1. For scalars and vectors with 10^{-5} eV $\lesssim m_X \lesssim 10^8$ eV, long-term NS cooling is by far the most sensitive probe (Table I). Energy loss through low-mass particles typically follows a power law T^p of

TABLE I. Stellar cooling bounds on the gauge or Yukawa coupling g of muonic bosons with mass $m_X \lesssim 1$ keV. The globular cluster (GC) bound comes from the limit on $G_{X\gamma\gamma}$ through a muon loop.

	Pseudo	Scalar	Vector
NS cooling (new)	2.9×10^{-9}	1.2×10^{-12}	2.8×10^{-13}
SN 1987A cooling [22] ^a	9.1×10^{-9}	4.2×10^{-9}	2.7×10^{-9}
GC stars [22] ^b	2.6×10^{-9}	3.9×10^{-9}	—

^aConservative bounds from the cold SN model.

^bUpdated to new ALP bound from GC stars [32].

internal NS temperature. Neutrino cooling by modified Urca (murca) emission, e.g. $nn \rightarrow npe^- \bar{\nu}_e$, has $p = 8$ [25, 26], whereas axion emission $NN \rightarrow NN a$ has $p = 6$ [27–29]. Therefore, as T decreases, axion cooling can dominate at late times, allowing one to set constraints on the axion-nucleon coupling [27–29]. These and the SN 1987A cooling bounds are nearly identical [30], implying that for any process with $p < 6$, NS cooling is more sensitive, as the new channel would affect the system even more strongly at late times. For instance, some of us have previously considered baryophilic bosons, where emission rates scale as T^4 , and found that the cooling of middle-aged NSs is far more sensitive than SN 1987A [28, 31]. For masses 10^{-11} eV $\lesssim m_X \lesssim 10^{-5}$ eV, long-range forces could affect the hydrostatic equilibrium, so new interactions should be weaker than gravity to avoid modifying the structure of neutron stars.

Essentials of NS cooling—After formation in stellar core collapse, a NS cools by neutrinos for about 10^5 years, at which point photons take over. The mechanical NS structure is set by degenerate matter, largely decoupled from thermal properties, characterized by the temperature T of the isothermal core. Its heat capacity is proportional to T , set by degenerate matter, and so its internal energy is

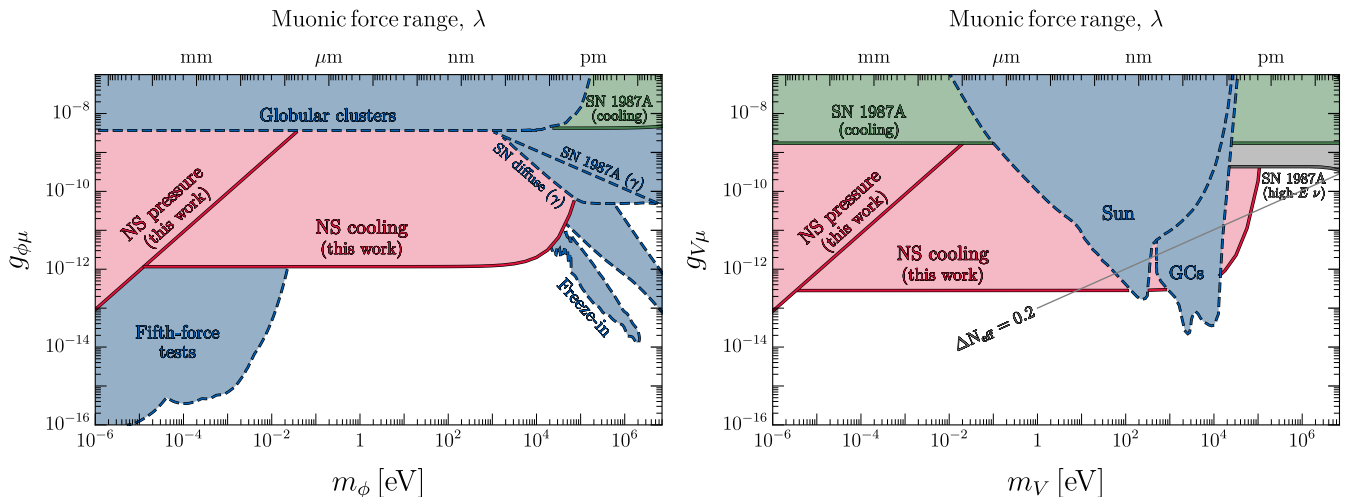


FIG. 1. Bounds on the coupling of muonic scalars (*left*) and vectors (*right*) as a function of their mass m_X , or force range $\lambda = 1/m_X$ (upper axis). Solid lines derive from tree-level couplings, dashed ones from loop-level interactions. The supernova (SN) and globular cluster (GC) bounds on scalars are from Ref. [22] with updates from [32], while bounds from an irreducible cosmological scalar population are from [33]. We obtain fifth-force bounds through the loop-induced coupling to protons (see text). For vectors, we show additional constraints arising from a coupling to muon neutrinos; the SN 1987A bounds from cooling and from nonobservation of high-energy neutrinos are from Ref. [24], while the solar and GC bounds are scaled from existing ones on dark photons [34, 35]. For couplings along the gray line, neutrino coalescence into V and the subsequent decay of the latter result in $\Delta N_{\text{eff}} = 0.2$ [36].

$U = C_U T^2$. The neutrino luminosity scales as $L_\nu = C_\nu T^8$, implying $T \propto t^{-1/6}$. Moreover, the photon luminosity follows $L_\gamma \propto T_s^4$ in terms of the surface temperature. The latter can be related to T of the core through the heat flux transported by degenerate heat carriers with a conductivity proportional to T . Therefore, the heat flux is $\propto T^2$ and radiated away $\propto T_s^4$ according to the Stefan-Boltzmann law. Hence, $T_s \propto T^{1/2}$, so that $L_\gamma = C_\gamma T^2 \propto t^{-1/3}$ during neutrino cooling. When photon cooling takes over, since both U and L_γ scale as T^2 , one finds $L_\gamma \propto e^{-t/\tau}$ with τ about 10^6 years.

This simple description agrees with a numerical reference model detailed in the End Matter and illustrated in Fig. 2. It shows the evolution of L_γ , L_ν , and T , both from the numerical model (thick solid lines) and from the analytic description (dashed lines) with parameters chosen to fit the numerical model, specifically $C_\nu = 1.06$ and $C_\gamma = 1.27$ (luminosities in 10^{33} erg s^{-1} , T in 10^8 K), and $\tau = 7 \times 10^5$ years. Neutrino-photon equality occurs at around 7×10^4 years with internal $T \simeq 8.9$ keV and $L_\nu = L_\gamma \simeq 1.4 \times 10^{33}$ erg s^{-1} .

General particle bounds—These results would be modified by a new cooling channel $L_X = C_X T^p$. For a baryophilic scalar ($p = 4$) [28, 31], we show $L_\phi(t)$ in Fig. 2 with C_ϕ adjusted such that it intersects the point where $L_\nu = L_\gamma$ of the unperturbed NS model. We also show the modified cooling history when L_ϕ is self-consistently included (thin solid lines). Such a cooling channel, that becomes important only at late times, simply shortens the cooling time. It is therefore clear that, if $2 < p < 8$, the impact of the new cooling channel is most pronounced

at neutrino-photon equality.

Realistic NS evolution is a complicated subject because of uncertainties of the nuclear Equation of State (EoS), the possibility of nucleon superfluidity or other novel phases, the associated uncertainty of the neutrino emissivities, the role of strong B fields, and of course the overall uncertain stellar parameters. Despite these complications, one could follow Refs. [29, 31], who considered some of the magnificent seven NSs and PSR J0659, and compared their measured ages and luminosities with cooling models calculated with the public code NSCool [37]. It allows one to switch between different EoSs and different assumptions about neutron and proton superfluidity. For a new cooling channel, one can then adjust these parameters and the NS mass, and after marginalization over these nuisance parameters, constrain the new energy loss.

For both axions [29] and baryophilic bosons [31], the resulting constraint is driven by the pulsar J1605 with age and luminosity shown in Fig. 2. Using the standard EoS APR [38] without superfluidity, the best-fit baryonic mass of the unperturbed model is then $1.8 M_\odot$, which is our reference NS, with more detailed properties shown in the End Matter. Using the improved neutrino rates of Bottaro et al. [26] instead of those of Friman and Maxwell [25] makes the standard cooling curve in Fig. 2 match even better with J1605.

For baryophilic scalars, the full statistical analysis yields $g_N \lesssim 5 \times 10^{-14}$ at 95% CL for the coupling to nucleons [31]. At this coupling strength and for conditions of photon-neutrino equality of our reference star, $L_\phi = 3.7 \times 10^{32}$ erg s^{-1} . Therefore, the limit can be recovered by the

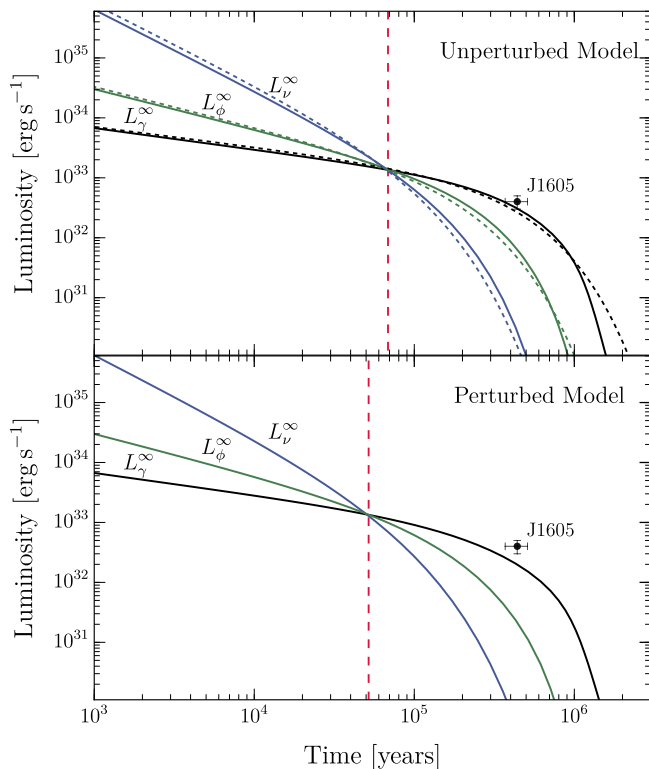


FIG. 2. Evolution of L_γ (black), L_ν (blue) and L_ϕ (green) in our reference NS model simulated with `NSCool`, where ϕ is a baryophilic scalar with $g_{\phi N} \simeq 9.5 \times 10^{-14}$, saturating the NS cooling criterion (see text). The observed NS is J1605. *Upper panel:* Unperturbed model, dashed lines showing the analytic scalings of L_γ , L_ν and L_ϕ . Here, L_ϕ derives from post-processing the unperturbed model. *Lower panel:* L_ϕ is self-consistently included in `NSCool` as a new cooling channel. The red dashed lines indicate the epochs when the different cooling channels become equal, which occurs at $T_{\text{core}} \simeq 8.9$ keV.

simple requirement $L_\phi \lesssim 0.3 L_\nu$ at $T = 8.9$ keV.

In other words, the intuitive requirement $L_X \lesssim L_\nu$ for a new cooling channel, evaluated at neutrino-photon equality, provides an excellent criterion, which in the baryophilic case is actually rather conservative. On the other hand, the modest gain of a detailed analysis lies well within astrophysical uncertainties. We therefore adopt this schematic condition as our NS cooling criterion to constrain muonic bosons. Equivalently, for an average NS baryonic density of $\sim 8.5 \times 10^{14}$ g cm $^{-3}$, the new bosons should obey

$$\epsilon_X \lesssim 0.3 \text{ erg g}^{-1} \text{ s}^{-1} \quad (1)$$

to avoid overly fast NS cooling. This approximate bound does not strongly depend on the power-law index p and essentially coincides with Iwamoto's original criterion [27].

Muonic boson emission—The main challenge is now to compute bremsstrahlung production through muons scattering electromagnetically off protons, other muons, and electrons. As the NS interior hosts similar populations

of these charged fermions, all of these channels contribute with comparable strength.

While electromagnetic interactions do not suffer from nuclear physics uncertainties [39], they are screened. Since the participating particles are at least semi-relativistic, the interaction is mediated by both longitudinal and transverse photons. While the former are screened at the Thomas-Fermi scale, transverse excitations can be screened or damped, depending on whether protons are superconducting or not [40–42]. Moreover, the phase space of degenerate particles constrains collisions to be mostly forward, a regime suppressed by screening, which thus enters linearly in the denominator, not logarithmically, resulting in significant uncertainties.

In-medium effects further complicate the precise evaluation of emissivities [43, 44]. For a purely muonic vector boson, the effective coupling to muons is somewhat suppressed, while an effective coupling to electrons is generated. Because electrons are much more relativistic, they radiate the main flux of muonic vectors.

We defer a detailed study of the emission rates to a technical companion paper [45] and here only provide intuitive scaling arguments. We focus on muon bremsstrahlung of scalars, $\mu\mu \rightarrow \mu\mu\phi$, since the same reasoning pertains to vectors and pseudoscalars. Soft quanta with $\omega \sim T$ can be treated as classical radiation. We here rely on non-relativistic muons, whereas in Ref. [45] we extend to the relativistic case.

The scalar field is sourced by a current proportional to the change in velocity of the radiating particle, providing an emission amplitude per particle proportional to $g_{\phi\mu}\Delta v$. Here, $\Delta v = q/\mu_\mu$ is the velocity change in terms of the chemical potential μ_μ and the exchanged momentum $|\mathbf{q}|$, which is comparable to the Meissner scale m_M in the superconducting regime, or Landau damping scale m_Λ in the non-superconducting regime. Hence, the matrix element for bremsstrahlung emission \mathcal{M}_ϕ relates to the one for the scattering $\mathcal{M}_{\mu\mu \rightarrow \mu\mu}$ through

$$\mathcal{M}_\phi \sim \frac{g_{\phi\mu} m_M}{\omega \mu_\mu} \mathcal{M}_{\mu\mu \rightarrow \mu\mu}, \quad (2)$$

where ω^{-1} is the characteristic factor for bremsstrahlung emission. Integrating the radiated energy ω over the squared amplitude and the phase space $d^3\mathbf{k}/[(2\pi)^3 2\omega]$, and considering that factors $\omega \sim k$ are of order T , the total radiated energy per unit time and volume is

$$Q_\phi \sim \frac{g_{\phi\mu}^2 T m_M^2}{\mu_\mu^2} n_\mu^2 \sigma_{\mu\mu} F_{\text{deg}}, \quad (3)$$

where $n_\mu \sim \mu_\mu^3$ is the muon density and $\sigma_{\mu\mu} \sim \alpha^2/m_M^2$ the cross section of muon-muon scattering through transverse photon exchange.

To estimate the degeneracy suppression F_{deg} , we note that incoming particles participate only if their momentum transverse to the Fermi surface lies in a thin shell

of relative size T/μ_μ . The final-state particles are completely constrained by energy-momentum conservation, while degeneracy allows the other's momentum to change only by an amount of order T transverse to the Fermi surface, whereas in the nondegenerate case it would be of the order of $q \sim m_M$. Overall, $F_{\text{deg}} \sim T^3/\mu_\mu^2 m_M$ and the scale for the energy-loss rate per unit volume is

$$Q_\phi \sim \frac{g_{\phi\mu}^2 \alpha^2 \mu_\mu^2 T^4}{m_M}. \quad (4)$$

The same scaling pertains to vector bosons. In a non-superconducting medium, the Meissner mass should be replaced with the Landau damping scale $m_\Lambda \sim (\alpha\mu_\mu^2 T)^{1/3}$.

Therefore, for both scalars and vectors, the emission rate from non-superconducting matter scales as $L_X = C_X T^{11/3}$, with the same units as before. For our unperturbed reference NS model, at photon-neutrino equality, we find numerically $C_\phi = 9 \times 10^{23} g_{\phi\mu}^2$ for scalars and $C_V = 1.5 \times 10^{25} g_{V\mu}^2$ for vectors. NS cooling then immediately yields the limits on the Yukawa couplings of muonic scalars and vectors ($m_X \lesssim 100$ keV) shown in Table I and Fig. 1, that are 3–4 orders of magnitude more stringent than SN 1987A cooling bounds.

For completeness, we also consider a pseudoscalar structure for which the scattering amplitude is

$$\mathcal{M}_a \sim \frac{g_{a\mu} k m_M}{\omega \mu_\mu^2} \mathcal{M}_{\mu\mu \rightarrow \mu\mu}. \quad (5)$$

Pseudoscalar emission then scales as $L_a = C_a T^{17/3}$, with $C_a = 1.3 \times 10^{17} g_{a\mu}^2$, and NS cooling implies $g_{a\mu} \gtrsim 6.7 \times 10^{-9}$, a limit similar to the SN 1987A cooling bound [22] as mentioned earlier.

Long-range forces in neutron stars—Low-mass bosons exert long-range forces between muon-rich bodies (attractive for scalars, repulsive for vectors), affecting binary NS evolution and gravitational-wave emission [18, 19] if the Compton wavelength exceeds around 10 km. During a NS merger with a black hole (BH), muonic bosons would be abundantly emitted, modifying the gravitational wave signature. In a NS-NS merger, an additional long-range force appears between the two components.

In the massless limit, the new force is completely set by $g_{X\mu} Y_\mu$. For a muon fraction $Y_\mu = 0.04$, the new interaction exceeds the gravitational one unless $g_{X\mu} \lesssim m_\mu/Y_\mu M_{\text{Pl}} \sim 10^{-18}$, where M_{Pl} is Planck mass. Stronger bounds of $g_{X\mu} \lesssim 10^{-20}$ ensue to avoid anomalously fast orbital decay of binary pulsars [19]. Yet smaller couplings ($g_{X\mu} \simeq 10^{-21}$) could be probed by LIGO through the detection of gravitational wave signals from NS-NS or BH-NS mergers [19]. Finally, for certain mass ranges around 10^{-20} and 10^{-11} eV, muonic bosons are sensitive to superradiance constraints from supermassive BHs [46].

Even for a Compton wavelength smaller than the NS radius, the muonic force can still compete with gravity by contributing to local pressure, affecting hydrostatic

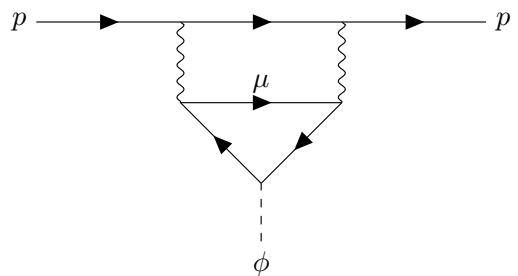


FIG. 3. Two-loop muonic scalar interaction with protons.

equilibrium. Hence, we require the muonic pressure to be smaller than the gravitational one. To ensure stability of a NS with mass M_{NS} and radius R_{NS} we thus require

$$P_\mu \simeq 4\pi g_{X\mu}^2 \frac{n_\mu^2}{m_X^2} \lesssim \frac{M_{\text{NS}}^2}{m_{\text{Pl}}^2 R_{\text{NS}}^4}. \quad (6)$$

Fig. 1 reveals that this constraint surpasses the NS cooling bounds for $m_X \lesssim 10^{-5}$ eV.

Comparison to previous bounds—The cooling speed of the nascent NS in SN 1987A, measured by the neutrino signal [47], constrains all interaction structures, predominantly through $\gamma\mu \rightarrow \mu X$ [22]. These tree-level constraints are shown as solid green lines in Fig. 1, and apply to both scalars and vectors.

Additional constraints arise from loop-level interactions, shown as dashed lines in Fig. 1. In particular, (pseudo)scalars acquire loop-induced two-photon couplings through a muon triangle loop. As a result, for $m_\phi \gtrsim 100$ keV, the most sensitive tests come from radiative decays of (pseudo)scalars emitted by SN 1987A and by all SNe in the universe [22], while for smaller masses, cooling arguments take over. Notably the globular cluster bound, $G_{\phi\gamma\gamma} < 0.47 \times 10^{-10} \text{ GeV}^{-1}$ [32], implies the updated limits shown in Table I.

Scalars decaying to photon pairs after leaving the NS may also contribute to the cosmic diffuse X-ray background (CXB) or give rise to an X-ray excess in the emission spectra from isolated NSs. However, we show in the Supplemental Material (SupM) [48] that constraints arising from X-ray observations are significantly weaker than those from NS cooling.

On the other hand, their loop-induced photon coupling allows scalars to couple to charged particles (Fig. 3). As shown in the SupM [48], the coupling to electrons is suppressed by powers of the small ratio m_e/m_μ , whereas the effective coupling to protons is

$$g_{\phi p} = \frac{\alpha^2}{2} g_{\phi\mu}. \quad (7)$$

Therefore, even ordinary matter is sensitive to muonic forces, which can violate the inverse-square law and the equivalence principle. Hence, fifth-force limits can be directly translated, yielding the constraints shown in Fig. 1.

Specifically, tests of deviations from the inverse-square law [1–10, 49–58] place severe limits on Yukawa couplings of muonic scalars with masses $m_\phi \lesssim 30$ meV, surpassing astrophysical bounds by many orders of magnitude.

An example of muonic vector is the gauge boson associated to $U(1)_{L_\mu-L_\tau}$. The latter can mix with the Standard Model photon through a loop of charged leptons, generating a coupling $\frac{\epsilon}{2} F^{\mu\nu} X_{\mu\nu}$, with $\epsilon \simeq -g_{V\mu}/70$. Therefore, astrophysical constraints on dark photons can be directly rescaled [34, 35]. On the other hand, fifth-force bounds do not apply to dark photons. Therefore, muonic forces mediated by vectors could be probed only, e.g., through tests of Coulomb’s law [59, 60], but the resulting limits can never compete with astrophysical ones. Additional constraints arise from the coupling to neutrinos. For large masses, the particle could decay back into neutrinos en-route to Earth, producing a high-energy neutrino flux that was not observed by Kamiokande II and IMB in correspondence to the SN 1987A event [24, 61].

Finally, neutrinos in the early Universe can coalesce into V , whose subsequent delayed decay can inject energetic neutrinos, resulting in a non-zero contribution to the effective number of neutrino species, ΔN_{eff} [36]. To have an impact on the cosmic microwave background, V must be heavier than twice the lightest neutrino [62], and it must decay before photon decoupling. Therefore, in Fig. 1 we show $\Delta N_{\text{eff}} = 0.2$ only down to $m_V = 1$ eV.

Discussion and outlook—The large muon populations in NSs provide unique probes of novel bosons coupled to second-generation leptons, both through NS cooling and additional pressure caused by the muonic force. The resulting bounds surpass previous sensitivity by many orders of magnitude (Fig. 1). One exception to our original premise that a large muon population was needed consists of fifth-force constraints on scalars, based on ordinary matter, that arise from a loop-induced muonic force on protons.

This work can be expanded in several directions that we plan to explore in future. Although we have obtained an approximate constraint from hydrostatic equilibrium, preliminary estimates suggest that much larger regions of parameter space can be probed by an analysis of the NS structure. LIGO observations of NS-NS mergers similar to GW170817 [63–66], as well as additional data from NICER [67, 68], will significantly strengthen our knowledge of the EoS [69, 70], contextually probing any deviation due to fifth forces.

In our NS cooling results we have assumed the APR EoS. However, asymmetric and β -stable nuclear matter could feature Σ^- and Λ hyperons [71, 72]. While the resulting reduction in the muon density affects our result only marginally (the charged lepton population is suppressed only at densities exceeding $\sim 8 \times 10^{14}$ g/cm³), the presence of hyperons, which contain second generation quarks, could result in more stringent constraints on fifth forces coupling to the latter, with possible consequences on

the allowed parameter space of dark matter interacting through a light mediator [73].

Acknowledgments—This article is based upon work from COST Action COSMIC WISPerS (CA21106), supported by COST (European Cooperation in Science and Technology). GGR acknowledges partial support by the German Research Foundation (DFG) through the Collaborative Research Centre “Neutrinos and Dark Matter in Astro- and Particle Physics (NDM),” Grant SFB–1258–283604770 and under Germany’s Excellence Strategy through the Cluster of Excellence ORIGINS EXC–2094–390783311. EV acknowledges support by the Italian MUR Departments of Excellence grant 2023–2027 “Quantum Frontier”. AL, NS and EV are supported by the Italian MUR through the FIS 2 project FIS–2023–01577 (DD n. 23314 10–12–2024, CUP C53C24001460001), and by Istituto Nazionale di Fisica Nucleare (INFN) through the Theoretical Astroparticle Physics (TAsP) project.

-
- [1] A. O. Sushkov, W. J. Kim, D. A. R. Dalvit and S. K. Lamoreaux, *New Experimental Limits on Non-Newtonian Forces in the Micrometer Range*, *Phys. Rev. Lett.* **107** (2011) 171101 [1108.2547].
 - [2] Y. J. Chen, W. K. Tham, D. E. Krause, D. Lopez, E. Fischbach and R. S. Decca, *Stronger Limits on Hypothetical Yukawa Interactions in the 30–8000 nm Range*, *Phys. Rev. Lett.* **116** (2016) 221102 [1410.7267].
 - [3] A. A. Geraci, S. J. Smullin, D. M. Weld, J. Chiaverini and A. Kapitulnik, *Improved constraints on non-Newtonian forces at 10 microns*, *Phys. Rev. D* **78** (2008) 022002 [0802.2350].
 - [4] D. J. Kapner, T. S. Cook, E. G. Adelberger, J. H. Gundlach, B. R. Heckel, C. D. Hoyle and H. E. Swanson, *Tests of the gravitational inverse-square law below the dark-energy length scale*, *Phys. Rev. Lett.* **98** (2007) 021101 [hep-ph/0611184].
 - [5] J. G. Lee, E. G. Adelberger, T. S. Cook, S. M. Fleischer and B. R. Heckel, *New Test of the Gravitational $1/r^2$ Law at Separations down to 52 μm* , *Phys. Rev. Lett.* **124** (2020) 101101 [2002.11761].
 - [6] G. L. Smith, C. D. Hoyle, J. H. Gundlach, E. G. Adelberger, B. R. Heckel and H. E. Swanson, *Short range tests of the equivalence principle*, *Phys. Rev. D* **61** (2000) 022001 [2405.10982].
 - [7] S.-Q. Yang, B.-F. Zhan, Q.-L. Wang, C.-G. Shao, L.-C. Tu, W.-H. Tan and J. Luo, *Test of the Gravitational Inverse Square Law at Millimeter Ranges*, *Phys. Rev. Lett.* **108** (2012) 081101.
 - [8] W.-H. Tan et al., *Improvement for Testing the Gravitational Inverse-Square Law at the Submillimeter Range*, *Phys. Rev. Lett.* **124** (2020) 051301.
 - [9] J. K. Hoskins, R. D. Newman, R. Spero and J. Schultz, *Experimental tests of the gravitational inverse square law for mass separations from 2-cm to 105-cm*, *Phys. Rev. D* **32** (1985) 3084.
 - [10] J. Bergé, P. Brax, G. Métris, M. Pernot-Borràs, P. Touboul and J.-P. Uzan, *MICROSCOPE Mission: First Constraints on the Violation of the Weak*

- Equivalence Principle by a Light Scalar Dilaton, *Phys. Rev. Lett.* **120** (2018) 141101 [1712.00483].
- [11] R. Foot, *New Physics From Electric Charge Quantization?*, *Mod. Phys. Lett. A* **6** (1991) 527.
- [12] X. G. He, G. C. Joshi, H. Lew and R. R. Volkas, *New- Z' phenomenology*, *Phys. Rev. D* **43** (1991) 22.
- [13] X.-G. He, G. C. Joshi, H. Lew and R. R. Volkas, *Simplest Z' model*, *Phys. Rev. D* **44** (1991) 2118.
- [14] R. Foot, X. G. He, H. Lew and R. R. Volkas, *Model for a light Z' boson*, *Phys. Rev. D* **50** (1994) 4571 [hep-ph/9401250].
- [15] B. Batell, A. Freitas, A. Ismail and D. Mckeen, *Flavor-specific scalar mediators*, *Phys. Rev. D* **98** (2018) 055026 [1712.10022].
- [16] B. Batell, A. Freitas, A. Ismail, D. McKeen and M. Rai, *Renormalizable models of flavor-specific scalars*, *Phys. Rev. D* **104** (2021) 115032 [2107.08059].
- [17] L. Di Luzio, M. Giannotti, E. Nardi and L. Visinelli, *The landscape of QCD axion models*, *Phys. Rept.* **870** (2020) 1 [2003.01100].
- [18] T. Kumar Poddar, S. Mohanty and S. Jana, *Vector gauge boson radiation from compact binary systems in a gauged $L_\mu - L_\tau$ scenario*, *Phys. Rev. D* **100** (2019) 123023 [1908.09732].
- [19] J. A. Dror, R. Laha and T. Opferkuch, *Probing muonic forces with neutron star binaries*, *Phys. Rev. D* **102** (2020) 023005 [1909.12845].
- [20] R. Bollig, W. DeRocco, P. W. Graham and H.-T. Janka, *Muons in Supernovae: Implications for the Axion-Muon Coupling*, *Phys. Rev. Lett.* **125** (2020) 051104 [2005.07141]. Erratum *Phys. Rev. Lett.* **126**, 189901 (2021).
- [21] D. Croon, G. Elor, R. K. Leane and S. D. McDermott, *Supernova Muons: New Constraints on Z' Bosons, Axions and ALPs*, *JHEP* **01** (2021) 107 [2006.13942].
- [22] A. Caputo, G. Raffelt and E. Vitagliano, *Muonic boson limits: Supernova redux*, *Phys. Rev. D* **105** (2022) 035022 [2109.03244].
- [23] K. Akita, S. H. Im, M. Masud and S. Yun, *Limits on heavy neutral leptons, Z' bosons and majorons from high-energy supernova neutrinos*, *JHEP* **07** (2024) 057 [2312.13627].
- [24] N. Blinov, P. J. Fox, K. J. Kelly, R. Plestid and T. Zhou, *$L_\mu - L_\tau$ gauge bosons in beam dumps and supernovae*, **2511.09619**.
- [25] B. L. Friman and O. V. Maxwell, *Neutron Star Neutrino Emissivities*, *Astrophys. J.* **232** (1979) 541.
- [26] S. Bottaro, A. Caputo and D. F. G. Fiorillo, *Neutrino emission in cold neutron stars: Bremsstrahlung and modified urca rates reexamined*, *JCAP* **11** (2024) 015 [2406.18640].
- [27] N. Iwamoto, *Axion Emission from Neutron Stars*, *Phys. Rev. Lett.* **53** (1984) 1198.
- [28] N. Ishizuka and M. Yoshimura, *Axion and Dilaton Emissivity from Nascent Neutron Stars*, *Prog. Theor. Phys.* **84** (1990) 233.
- [29] M. Buschmann, C. Dessert, J. W. Foster, A. J. Long and B. R. Safdi, *Upper Limit on the QCD Axion Mass from Isolated Neutron Star Cooling*, *Phys. Rev. Lett.* **128** (2022) 091102 [2111.09892].
- [30] A. Caputo and G. Raffelt, *Astrophysical Axion Bounds: The 2024 Edition*, *PoS COSMICWISPerS* (2024) 041 [2401.13728].
- [31] D. F. G. Fiorillo, A. Lella, C. A. J. O'Hare and E. Vitagliano, *Leading Bounds on Micrometer to Picometer Fifth Forces from Neutron Star Cooling*, *Phys. Rev. Lett.* **135** (2025) 211003 [2506.19906].
- [32] M. J. Dolan, F. J. Hiskens and R. R. Volkas, *Advancing globular cluster constraints on the axion-photon coupling*, *JCAP* **10** (2022) 096 [2207.03102].
- [33] K. Langhoff, N. J. Outmezguine and N. L. Rodd, *Irreducible Axion Background*, *Phys. Rev. Lett.* **129** (2022) 241101 [2209.06216].
- [34] S.-P. Li and X.-J. Xu, *Production rates of dark photons and Z' in the Sun and stellar cooling bounds*, *JCAP* **09** (2023) 009 [2304.12907].
- [35] M. J. Dolan, F. J. Hiskens and R. R. Volkas, *Constraining dark photons with self-consistent simulations of globular cluster stars*, *JCAP* **05** (2024) 099 [2306.13335].
- [36] M. Escudero, D. Hooper, G. Krnjaic and M. Pierre, *Cosmology with A Very Light $L_\mu - L_\tau$ Gauge Boson*, *JHEP* **03** (2019) 071 [1901.02010].
- [37] D. Page, *NSCool: Neutron star cooling code*, Astrophysics Source Code Library, record ascl:1609.009, Sept., 2016.
- [38] A. Akmal, V. R. Pandharipande and D. G. Ravenhall, *The Equation of state of nucleon matter and neutron star structure*, *Phys. Rev. C* **58** (1998) 1804 [nucl-th/9804027].
- [39] D. F. G. Fiorillo, T. Pitik and E. Vitagliano, *Supernova production of axionlike particles coupling to electrons, reloaded*, *Phys. Rev. D* **112** (2025) 083008 [2503.15630]. Erratum: *Phys. Rev. D* **113** (2026) 089902.
- [40] P. S. Shternin and D. G. Yakovlev, *Electron-muon heat conduction in neutron star cores via the exchange of transverse plasmons*, *Phys. Rev. D* **75** (2007) 103004 [0705.1963].
- [41] P. S. Shternin and D. G. Yakovlev, *Electron thermal conductivity owing to collisions between degenerate electrons*, *Phys. Rev. D* **74** (2006) 043004 [astro-ph/0608371].
- [42] P. S. Shternin, *Neutrino-Pair Bremsstrahlung Due to Electromagnetic Collisions in Neutron Star Cores Revisited*, *Particles* **8** (2025) 100 [2512.08780].
- [43] L. B. Leinson and A. Perez, *Collective effects in neutrino anti-neutrino synchrotron radiation from neutron stars*, *Phys. Rev. D* **59** (1999) 043002 [astro-ph/9710257].
- [44] L. B. Leinson, *Neutrino pair emission due to electron phonon scattering in a neutron star crust: A reappraisal*, *Phys. Lett. B* **469** (1999) 166 [hep-ph/0009049].
- [45] D. F. G. Fiorillo, A. Lella, G. G. Raffelt, N. Selimović and E. Vitagliano, *Production of Leptophilic Bosons in Ultradegenerate Relativistic Matter*, 2026. Work in Progress.
- [46] M. Baryakhtar, R. Lasenby and M. Teo, *Black Hole Superradiance Signatures of Ultralight Vectors*, *Phys. Rev. D* **96** (2017) 035019 [1704.05081].
- [47] D. F. G. Fiorillo, M. Heinlein, H.-T. Janka, G. Raffelt, E. Vitagliano and R. Bollig, *Supernova simulations confront SN 1987A neutrinos*, *Phys. Rev. D* **108** (2023) 083040 [2308.01403].
- [48] <https://>. See Supplemental Material for a discussion of possible constraints from scalar decays in photon pairs and details on our calculation for the loop-induced scalar coupling to protons.
- [49] R. S. Decca, D. Lopez, E. Fischbach, G. L. Klimchitskaya, D. E. Krause and V. M. Mostepanenko,

- Tests of new physics from precise measurements of the Casimir pressure between two gold-coated plates*, *Phys. Rev. D* **75** (2007) 077101 [[hep-ph/0703290](#)].
- [50] C. P. Blakemore, A. Fieguth, A. Kawasaki, N. Priel, D. Martin, A. D. Rider, Q. Wang and G. Gratta, *Search for non-Newtonian interactions at micrometer scale with a levitated test mass*, *Phys. Rev. D* **104** (2021) L061101 [[2102.06848](#)].
- [51] G. Venugopalan et al., *Optomechanical vector sensing of new forces at 6 micron separation*, *Sci. Rep.* **16** (2026) 5180 [[2412.13167](#)].
- [52] H. C. Chiu, G. L. Klimchitskaya, V. N. Marachevsky, V. M. Mostepanenko and U. Mohideen, *Demonstration of the asymmetric lateral Casimir force between corrugated surfaces in the nonadditive regime*, *Phys. Rev. B* **80** (2009) 121402 [[0909.2161](#)].
- [53] V. B. Bezerra, G. L. Klimchitskaya, V. M. Mostepanenko and C. Romero, *Advance and prospects in constraining the Yukawa-type corrections to Newtonian gravity from the Casimir effect*, *Phys. Rev. D* **81** (2010) 055003 [[1002.2141](#)].
- [54] A. A. Banishev, J. Wagner, T. Emig, R. Zandi and U. Mohideen, *Demonstration of Angle Dependent Casimir Force Between Corrugations*, *Phys. Rev. Lett.* **110** (2013) 250403 [[1212.6271](#)].
- [55] A. A. Banishev, J. Wagner, T. Emig, R. Zandi and U. Mohideen, *Experimental and theoretical investigation of the angular dependence of the Casimir force between sinusoidally corrugated surfaces*, *Phys. Rev. B* **89** (2014) 235436 [[1402.2716](#)].
- [56] J. E. J. Matias, A. S. Lemos and F. Dahia, *Probing short-distance modifications of gravity via spin-independent and spin-dependent effects in muonic atoms*, *Eur. Phys. J. Plus* **141** (2026) 328 [[2511.00719](#)].
- [57] J. Boynewicz and C. A. Sackett, *Probing short-range gravity using quantum reflection*, [2511.08770](#).
- [58] Y.-C. Ren, F. Xu, W. Broer, X.-J. Chen and F. Xue, *Field-Tunable Meissner-Levitated Ferromagnetic Microsphere Sensor for Cryogenic Casimir and Short-Range Gravity Tests*, [2602.13829](#).
- [59] D. F. Bartlett and S. Loegl, *Limits on an Electromagnetic Fifth Force*, *Phys. Rev. Lett.* **61** (1988) 2285.
- [60] D. Kroff and P. C. Malta, *Constraining hidden photons via atomic force microscope measurements and the Plimpton-Lawton experiment*, *Phys. Rev. D* **102** (2020) 095015 [[2008.02209](#)].
- [61] D. F. G. Fiorillo, G. G. Raffelt and E. Vitagliano, *Strong Supernova 1987A Constraints on Bosons Decaying to Neutrinos*, *Phys. Rev. Lett.* **131** (2023) 021001 [[2209.11773](#)].
- [62] KATRIN Collaboration, M. Aker et al., *Direct neutrino-mass measurement based on 259 days of KATRIN data*, *Science* **388** (2025) adq9592 [[2406.13516](#)].
- [63] LIGO SCIENTIFIC, VIRGO, FERMI GBM, INTEGRAL, ICECUBE, ASTROSAT CADMIUM ZINC TELLURIDE IMAGER TEAM, IPN, INSIGHT-HXMT, ANTARES, SWIFT, AGILE TEAM, 1M2H TEAM, DARK ENERGY CAMERA GW-EM, DES, DLT40, GRAWITA, FERMI-LAT, ATCA, ASKAP, LAS CUMBRES OBSERVATORY GROUP, OZGRAV, DWF (DEEPER WIDER FASTER PROGRAM), AST3, CAASTRO, VINROUGE, MASTER, J-GEM, GROWTH, JAGWAR, CALTECHNRAO, TTU-NRAO, NUSTAR, PAN-STARRS, MAXI TEAM, TZAC CONSORTIUM, KU, NORDIC OPTICAL TELESCOPE, ePESSTO, GROND, TEXAS TECH UNIVERSITY, SALT GROUP, TOROS, BOOTES, MWA, CALET, IKI-GW FOLLOW-UP, H.E.S.S., LOFAR, LWA, HAWC, PIERRE AUGER, ALMA, EURO VLBI TEAM, PI OF SKY, CHANDRA TEAM AT MCGILL UNIVERSITY, DFN, ATLAS TELESCOPES, HIGH TIME RESOLUTION UNIVERSE SURVEY, RIMAS, RATIR, SKA SOUTH AFRICA/MEERKAT Collaboration, B. P. Abbott et al., *Multi-messenger Observations of a Binary Neutron Star Merger*, *Astrophys. J. Lett.* **848** (2017) L12 [[1710.05833](#)].
- [64] LIGO SCIENTIFIC, VIRGO, FERMI-GBM, INTEGRAL Collaboration, B. P. Abbott et al., *Gravitational Waves and Gamma-rays from a Binary Neutron Star Merger: GW170817 and GRB 170817A*, *Astrophys. J. Lett.* **848** (2017) L13 [[1710.05834](#)].
- [65] LIGO SCIENTIFIC, VIRGO Collaboration, B. P. Abbott et al., *GW170817: Observation of Gravitational Waves from a Binary Neutron Star Inspiral*, *Phys. Rev. Lett.* **119** (2017) 161101 [[1710.05832](#)].
- [66] LIGO SCIENTIFIC, VIRGO Collaboration, B. P. Abbott et al., *Properties of the binary neutron star merger GW170817*, *Phys. Rev. X* **9** (2019) 011001 [[1805.11579](#)].
- [67] T. E. Riley et al., *A NICER View of PSR J0030+0451: Millisecond Pulsar Parameter Estimation*, *Astrophys. J. Lett.* **887** (2019) L21 [[1912.05702](#)].
- [68] M. C. Miller et al., *PSR J0030+0451 Mass and Radius from NICER Data and Implications for the Properties of Neutron Star Matter*, *Astrophys. J. Lett.* **887** (2019) L24 [[1912.05705](#)].
- [69] E. Burns, *Neutron Star Mergers and How to Study Them*, *Living Rev. Rel.* **23** (2020) 4 [[1909.06085](#)].
- [70] C. D. Capano, I. Tews, S. M. Brown, B. Margalit, S. De, S. Kumar, D. A. Brown, B. Krishnan and S. Reddy, *Stringent constraints on neutron-star radii from multimessenger observations and nuclear theory*, *Nature Astron.* **4** (2020) 625 [[1908.10352](#)].
- [71] M. Baldo, G. F. Burgio and H. J. Schulze, *Hyperon stars in the Brueckner-Bethe-Goldstone theory*, *Phys. Rev. C* **61** (2000) 055801 [[nucl-th/9912066](#)].
- [72] B. Bhat, A. Dohi, T. Muto and T. Noda, *Cooling of Isolated Neutron Stars with Hyperon-mixed Kaon-Condensation Matter*, [2605.09723](#).
- [73] S. Knapen, T. Lin and K. M. Zurek, *Light Dark Matter: Models and Constraints*, *Phys. Rev. D* **96** (2017) 115021 [[1709.07882](#)].
- [74] E. Vitagliano, I. Tamborra and G. Raffelt, *Grand Unified Neutrino Spectrum at Earth: Sources and Spectral Components*, *Rev. Mod. Phys.* **92** (2020) 45006 [[1910.11878](#)].
- [75] D. E. Gruber, J. L. Matteson, L. E. Peterson and G. V. Jung, *The spectrum of diffuse cosmic hard x-rays measured with HEAO-1*, *Astrophys. J.* **520** (1999) 124 [[astro-ph/9903492](#)].
- [76] R. Krivonos, D. Wik, B. Grefenstette, K. Madsen, K. Perez, S. Rosslund, S. Sazonov and A. Zoglauer, *NuSTAR measurement of the cosmic X-ray background in the 3–20 keV energy band*, *Mon. Not. Roy. Astron. Soc.* **502** (2021) 3966 [[2011.11469](#)].
- [77] N. Tetzlaff, J. G. Schmidt, M. M. Hohle and R. Neuhaeuser, *Neutron stars from young nearby associations the origin of RXJ1605.3+3249*, *Publ. Astron.*

Soc. Austral. **29** (2012) 98 [1202.1388].

- [78] F. Jansen, D. Lumb, B. Altieri, J. Clavel, M. Ehle, C. Erd, C. Gabriel, M. Guainazzi, P. Gondoin, R. Much, R. Munoz, M. Santos, N. Schartel, D. Texier and G. Vacanti, *XMM-Newton observatory. I. The spacecraft and operations*, *A&A* **365** (2001) L1.

- [79] XMM-Newton Science Operations Centre, *XMM-Newton Users Handbook: EPIC's sensitivity limits*, https://xmm-tools.cosmos.esa.int/external/xmm_user_support/documentation/uhb/epicsens.html. European Space Agency, XMM-Newton Users Handbook, Section 3.3.8; accessed 21 May 2026.

End Matter

Reference neutron star model—To illustrate the properties of medium-aged NSs used to constrain particle emission, we here show the properties of the NS model that best fits the observed age and luminosity of the pulsar J1605. The cooling lightcurves are calculated with the public code NSCool [37] by assuming the standard APR EoS without superfluidity, a NS mass $M_{\text{NS}} = 1.8 M_{\odot}$ and a fraction $\Delta M/M = 10^{-14}$ of light elements accreted

onto the NS envelope. The NS profile refers to the epoch when $L_{\nu} = L_{\gamma}$ which occurs at $t \simeq 7 \times 10^4$ years. The mass coordinate represents enclosed baryonic mass. All parameters are local quantities and as such relevant for the calculation of the emission rates. The core is very nearly isothermal, corresponding to variation of the local T according to the gravitational potential. In the main text, luminosities are those for a distant observer.

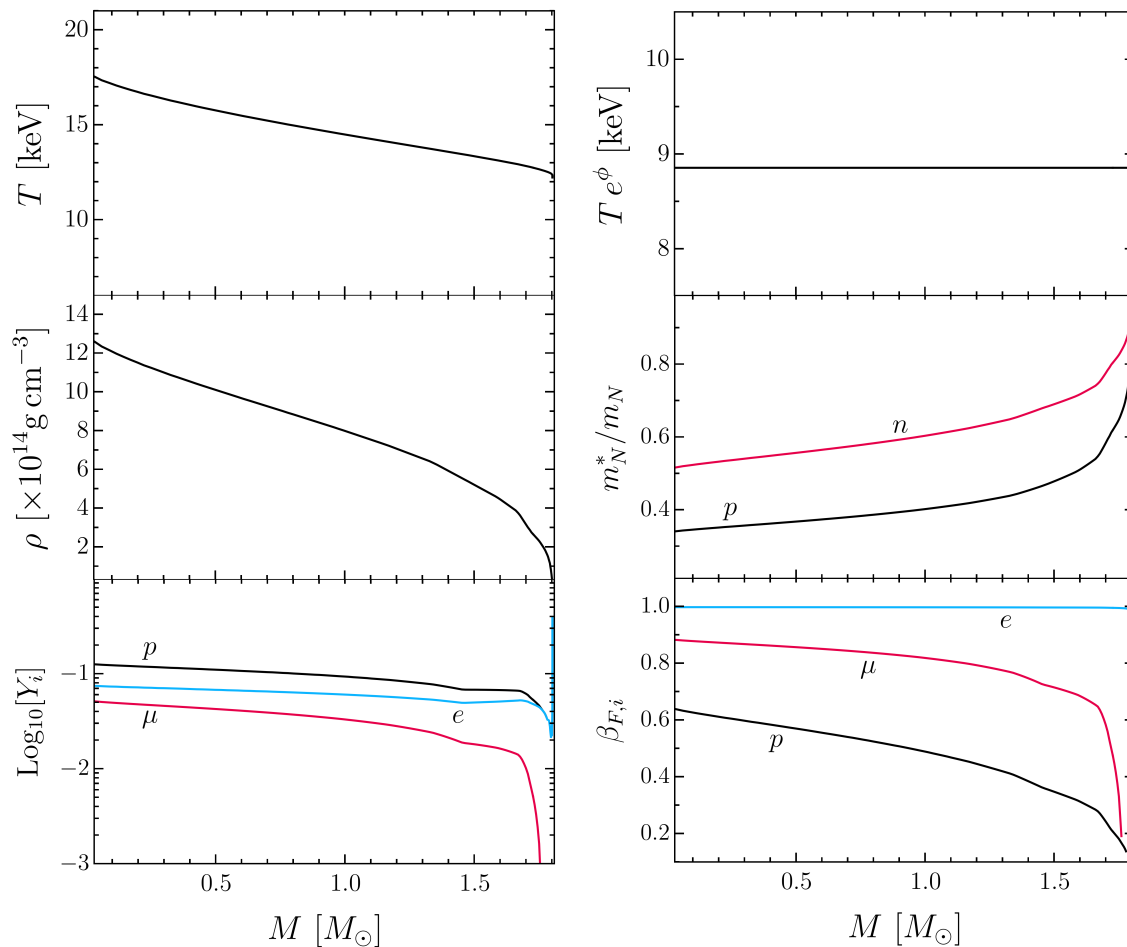


FIG. 4. Profile of our reference NS model at the epoch when $L_{\nu} = L_{\gamma}$, shown as a function of enclosed baryonic mass. The upper panels refer to the local temperature and the redshifted temperature as measured by a distant observer. The middle panels show the NS density and nucleon effective masses, while the lower panels report particle fractions and Fermi velocities of the charged species present in the stellar plasma.

Supplemental Material for the Letter

Neutron Star Bounds on Muonic Fifth Forces from Picometer to Kilometer Scales

In this Supplemental Material, we estimate possible constraints from scalar boson decays into photon pairs and detail our calculation for the loop-induced scalar coupling to protons.

A. Contribution to CXB

(Pseudo)scalars will decay to photon pairs after leaving the NS. To estimate their contribution to the cosmic X-ray background (CXB), we consider bosons with $L_\phi \propto T^p$, which are assumed to begin dominating over neutrinos at $t = t_0$, when $L_\gamma = L_\nu = L_0$. At earlier times, they are only a perturbative effect. During neutrino cooling, $T \propto t^{-1/6}$, and therefore $L_\phi = L_0(t/t_0)^{-p/6}$. The total energy emitted by bosons is $U_\phi = 6L_0t_0/(6-p)$.

We assume a Maxwell-Boltzmann spectrum at the NS internal temperature T , so the average ϕ energy is $3T$ and the number emission rate $\dot{N}_\phi = L_\phi/3T$. At photon-neutrino equality, $T = T_0$, and $T = T_0(t/t_0)^{-1/6}$ during neutrino cooling, so that $\dot{N}_\phi = (L_0/3T_0)(t/t_0)^{-(p-1)/6}$. Therefore, the total number of particles emitted is $N_\phi = [2/(7-p)]L_0t_0/T_0$ and the average particle energy is $\langle E_\phi \rangle = U_\phi/N_\phi = 3(7-p)T_0/(6-p)$. We approximate the integrated spectrum also as Maxwell-Boltzmann with $T_\phi = \langle E_\phi \rangle/3 = (7-p)T_0/(6-p)$.

After neutrino-photon equality, the NS cools mainly by photon emission and we conservatively neglect bosons emitted later, which also have smaller energies. As reference parameters we use $L_0 = 2 \times 10^{33}$ erg s $^{-1}$, $T_0 = 10^8$ K = 8.6 keV, and $t_0 = 0.7 \times 10^5$ years, implying $U_\phi = 1.65 \times 10^{55}$ keV/(6-p), $N_\phi = 6.4 \times 10^{53}/(7-p)$, and $\langle E_\phi \rangle = 3T_\phi = 25.8$ keV $(7-p)/(6-p)$.

The cosmic comoving density of all past core-collapse SNe was estimated in Eq. (40) of Ref. [74] as $n_{cc} = \xi_{cc} 10^7$ Mpc $^{-3}$, where $\xi_{cc} = 0.58$ –1.05, depending on the assumed star-formation rate. Ignoring BH-forming SNe, the cosmic average NS density is roughly identical with n_{cc} . The star formation rate was much larger in the past, so most NSs are very old. With $\xi_{cc} = 0.58$, the average cosmic density of the new particles is

$$n_\phi \simeq n_{cc} N_\phi \simeq 1.3 \times 10^{-13} \text{ cm}^{-3}/(7-p). \quad (\text{S1})$$

After multiplying with the speed of light, this is an isotropic flux of 3.8×10^{-3} cm $^{-2}$ s $^{-1}/(7-p)$. To obtain the directional flux, one needs to divide by 4π (see Appendix A of Ref. [74]) so that finally $d\Phi_\phi/d\Omega \simeq 3.0 \times 10^{-4}$ cm $^{-2}$ s $^{-1}$ sr $^{-1}/(7-p)$.

Assuming conservatively that all of the new particles decay into two photons until the present epoch, the γ spectrum normalized to 2 is

$$\frac{df_\gamma}{dE_\gamma} = \int_{E_\gamma}^{\infty} dE_\phi \frac{2}{E_\phi} \frac{df_\phi}{dE_\phi} = \frac{E_\gamma + T_\phi}{T_\phi^2} e^{-E_\gamma/T_\phi}, \quad (\text{S2})$$

assuming the original particles had a Maxwell-Boltzmann spectrum at temperature T_ϕ that was normalized to 1. The average photon energy is $\langle E_\gamma \rangle = 3T_\phi/2$ as expected. Most core-collapse SNe occur at cosmic redshift $z \simeq 1$, so for the normalized-to-2 present-day spectrum, we should use $T_\phi = T_{\phi, \text{emission}}/(1+z)$, in our case $T_\phi = \frac{1}{1+z} \times \frac{1}{3} \times 25.8$ keV $(7-p)/(6-p) \simeq 4.3$ keV $(7-p)/(6-p)$, implying $\langle E_\gamma \rangle \simeq 6.5$ keV $(7-p)/(6-p)$.

In terms of the present-day T_ϕ , the energy spectrum instead of the number spectrum is

$$S(E_\gamma) = \frac{d\Phi_\phi}{d\Omega} \frac{E_\gamma(E_\gamma + T_\phi)}{T_\phi^2} e^{-E_\gamma/T_\phi} \quad (\text{S3})$$

which has units keV keV $^{-1}$ cm $^{-2}$ s $^{-1}$ sr $^{-1}$. The CXB has been measured by several instruments. In the 3–60 keV range, an analytic formula was given by Gruber et al. [75],

$$S(E_\gamma) = 7.877 E_{\text{keV}}^{-0.29} e^{-E_{\text{keV}}/41.13} \frac{\text{keV}}{\text{keV cm}^2 \text{ s sr}}, \quad (\text{S4})$$

which seems to agree with the more recent NuSTAR measurements [76].

For $p = 4$, corresponding to a scalar boson, the maximum of the γ flux from particle decays of Eq. (S3) is around 1×10^{-4} smaller than the measurements at $E_\gamma \simeq 15$ keV, where the curves come closest. The situation is similar for $p = 4 - 1/3 = 11/3$ that pertains to emission in the normal-conducting phase.

For $p = 6$, corresponding to a pseudoscalar, the total energy U_ϕ formally diverges, due to a logarithmic contribution from early times. This points to the predominance of pseudoscalars emitted from the SN phase and one should not expect decay bounds from cold NSs to surpass those from SNe. Imposing a cut at an early time, where the temperature was a few hundred keV, modifies the above estimates only by a logarithmic factor of small relevance.

These generic estimates show that the CXB cannot constrain (pseudo)scalars beyond the NS cooling bounds.

B. Decays from isolated neutron stars

Scalars produced in nearby isolated NSs partly decay on their way to Earth, giving rise to an additional X-ray flux. To estimate this contribution, we take as an example our reference NS J1605 at a distance $D \simeq 350$ pc and age $t \simeq 4.4 \times 10^5$ years [77], that would have an internal $T \simeq 4$ keV in the frame of a distant observer.

The two-photon decay length of a scalar particle in the laboratory frame is

$$\lambda_{\phi\gamma\gamma} = \frac{64\pi E_\phi}{g_{\phi\gamma\gamma}^2 m_\phi^4} = \frac{144\pi^3 m_\mu^2 E_\phi}{g_{\phi\mu}^2 \alpha^2 m_\phi^4}, \quad (\text{S5})$$

where $g_{\phi\gamma\gamma} = 2\alpha g_{\phi\mu}/3\pi m_\mu$ is the loop-induced two-photon coupling of muon-philic scalars [22]. Numerically, at the cooling bound $g_{\phi\mu} = 10^{-12}$ and for $E_\phi = m_\phi = 10$ keV, we find $\lambda_{\phi\gamma\gamma} = 6 \times 10^{12}$ pc, much larger than the distance.

After the epoch of photon-neutrino equality, the temperature in the core decays exponentially with time $T \simeq T_0(t/t_0)^{-1/6} \exp[-t/\tau]$ in which $\tau \simeq 7 \times 10^5$, leading to $L_\phi \simeq L_0(t/t_0)^{-2/3} \exp(-4t/\tau) \exp(-m_\phi/T)$. In this expression, we accounted for an additional exponential suppression factor for the emission of bosons with masses $m_\phi \gtrsim T$. The rate of emitted particles at present is then estimated to $\dot{N}_\phi \simeq L_\phi/(m_\phi + 3T/2) \simeq 5.5 \times 10^{39} \text{ s}^{-1}$.

A very simple argument showing that decay bounds are rather weak is based on energetics. For a coupling equal to

the cooling bound, the present-day scalar luminosity from the NS is roughly $L_\gamma \simeq 3 \times 10^{31} \text{ erg/s}$. Therefore, the energy flux at Earth in the keV energy window ($E_\phi \sim 1$ keV) is roughly $\Phi_\phi \sim L_\gamma/4\pi D^2 E_\phi \sim 10^{-12} \text{ erg/s cm}^2 \text{ keV}$. A fraction $D/\lambda_{\phi\gamma\gamma}$ of this energy may have converted into visible X-rays, but as we have seen, this fraction is, even at a boson mass of $m_\phi = 10$ keV, rather small, of the order of 10^{-10} . For comparison, the sensitivity of XMM-Newton [78] reaches at most $10^{-16} \text{ erg/s cm}^2 \text{ keV}$ [79]. Hence, decays from isolated NSs are generally not a competitive probe compared with cooling.

C. Loop-induced couplings to protons

We consider the effective zero-momentum coupling of nonrelativistic nucleons to a scalar muonic boson. The amplitude, shown in the main text as Fig. 3, can be written as

$$-iF(K) = \lim_{K \rightarrow 0} \int \frac{d^4 Q}{(2\pi)^4} (-i\mathcal{T}^{\mu\nu}(K; K+Q, -Q)) \frac{16\pi^2 \alpha}{Q^2(Q+K)^2} [\gamma^\mu iG(P-Q)\gamma^\nu + \gamma^\nu iG(P+Q+K)\gamma^\mu]. \quad (\text{S6})$$

Here $G(P) = 1/(\not{P} - m_N)$ is the nucleon propagator, and $\mathcal{T}^{\mu\nu}(K; K+Q, -Q)$ denotes the muonic triangle loop amplitude. In the non-relativistic limit, we may only take the charge operator, so that $\mu = \nu = 0$, and replace the propagator by its non-relativistic form. Taking the limit $K \rightarrow 0$, the two propagators add to $-2\pi i\delta(Q^0)$ —a static field cannot carry energy. Therefore, after integrating the

delta function, this takes the much simpler form

$$-iF(K=0) = -i \int \frac{d^3 \mathbf{q}}{(2\pi)^3} \frac{16\pi^2 \alpha}{\mathbf{q}^4} \mathcal{T}^{00}[0; Q, -Q]. \quad (\text{S7})$$

We now discuss the triangle loop, whose general form is

$$-i\mathcal{T}^{\mu\nu}[0; Q, -Q] = -\alpha g_{\phi\mu} \int \frac{d^4 L}{(2\pi)^4} \left[\frac{\text{Tr}[\gamma^\mu(\not{L} + m_\mu)(\not{L} + m_\mu)\gamma^\nu(\not{L} - \not{Q} + m_\mu)]}{(L^2 - m_\mu^2)^2[(L-Q)^2 - m_\mu^2]} + (Q \rightarrow -Q) \right]. \quad (\text{S8})$$

The integral must satisfy Ward's identity, and therefore must take the form

$$\mathcal{T}^{\mu\nu} = T(Q^2)(Q^\mu Q^\nu - Q^2 g^{\mu\nu}). \quad (\text{S9})$$

By taking the trace of Eq. (S8), we then obtain

$$3iQ^2 T(Q^2) = -\alpha g_{\phi\mu} [\Phi(Q) + \Phi(-Q) - 2\Phi(0)] \quad (\text{S10})$$

with

$$\Phi(Q) = 16m_\mu \int \frac{d^4 L}{(2\pi)^4} \frac{m_\mu^2 + L \cdot Q}{(L^2 - m_\mu^2)^2[(L-Q)^2 - m_\mu^2]}. \quad (\text{S11})$$

Notice that the term $-2\Phi(0)$ was originally absent from our loop, and has been introduced to renormalize the result and remove the unphysical contact term for $Q \rightarrow 0$. The function $\Phi(Q)$ can now be deduced through the Feynman parameterization as

$$\Phi(Q) = -\frac{im_\mu}{\pi^2} \int_0^1 dx \frac{m_\mu^2 + (1-x)Q^2}{m_\mu^2 - x(1-x)Q^2}. \quad (\text{S12})$$

Therefore, we finally have

$$T(Q^2) = \frac{\alpha g_{\phi\mu} m_\mu}{\pi^2} \int_0^1 dx \frac{x(1-x)}{m_\mu^2 - x(1-x)Q^2}, \quad (\text{S13})$$

or explicitly performing the integral in Eq. (S8), one finds

$$T(Q^2) = g_{\phi\mu} \frac{\alpha}{4\pi} \frac{16m_\mu}{(Q^2 - 4m_\mu^2)Q^2} \left[4m_\mu^2 - Q^2 + \frac{2m_\mu^2 \sqrt{Q^2(Q^2 - 4m_\mu^2)}}{Q^2} \log \left(\frac{2m_\mu^2 - Q^2 + \sqrt{Q^2(Q^2 - 4m_\mu^2)}}{2m_\mu^2} \right) \right]. \quad (\text{S14})$$

Notice that this has a finite limit for $Q \rightarrow 0$.

After evaluating this for $Q^0 = 0$, we finally obtain the effective coupling $F(K = 0)$ as

$$\begin{aligned} g_{\phi p} &= F(K = 0) \\ &= 16\alpha^2 g_{\phi\mu} m_\mu \int \frac{d^3\mathbf{q}}{(2\pi)^3 \mathbf{q}^2} \int_0^1 dx \frac{x(1-x)}{m_\mu^2 + x(1-x)\mathbf{q}^2} \\ &= \frac{1}{2} g_{\phi\mu} \alpha^2. \end{aligned} \quad (\text{S15})$$

D. Loop-induced couplings to electrons

Let us also consider the effective coupling induced to electrons. In this case, we must abandon the nonrelativistic approximation for the electron propagator; even if the interacting electrons are nonrelativistic, the momentum Q flowing through them can reach up to the mass of the muon, much larger than that of the electron. Thus, we must use the full four-dimensional structure of the tensor $\mathcal{T}^{\mu\nu}$, but we can still take the limit $K \rightarrow 0$ and then obtain

$$F(K = 0) = i \int \frac{d^4Q}{(2\pi)^4} \frac{16\pi^2 \alpha T(Q^2) (Q_\mu Q_\nu - g_{\mu\nu} Q^2)}{Q^4} \left[\frac{\gamma^\mu (\not{P} - \not{Q} + m_e) \gamma^\nu}{-2P \cdot Q + Q^2 + i\epsilon} + (Q \leftrightarrow -Q) \right]. \quad (\text{S16})$$

In contracting with the tensor $Q^\mu Q^\nu - Q^2 g^{\mu\nu}$, we obtain

$$F(K = 0) = i \int \frac{d^4Q}{(2\pi)^4} \frac{16\pi^2 \alpha T(Q^2)}{Q^4} \left[\frac{Q^2 \not{P} + 2(P \cdot Q - Q^2) \not{Q} - 3m_e Q^2}{-2P \cdot Q + Q^2 + i\epsilon} + (Q \leftrightarrow -Q) \right]. \quad (\text{S17})$$

Since we are only interested in the action of this operator on the spinor of an electron on shell, we may replace $\not{P} \rightarrow m_e$. Furthermore, the integral of $\int Q^\mu F(Q^2, P \cdot Q) d^4Q \propto P^\mu$, so we may effectively replace $\not{Q} \rightarrow (Q \cdot P) \not{P} / m_e^2 \rightarrow (Q \cdot P) / m_e$. Thus, we finally obtain

$$F(K = 0) = i \int \frac{d^4Q}{(2\pi)^4} \frac{16\pi^2 \alpha T(Q^2)}{Q^2 m_e} \left[\frac{2m_e^2 + P \cdot Q}{2P \cdot Q - Q^2 - i\epsilon} - \frac{2m_e^2 - P \cdot Q}{2P \cdot Q + Q^2 + i\epsilon} \right]. \quad (\text{S18})$$

The integral is in a form that can be performed explicitly. However, we do not actually need to. It suffices to note that, differently from the nucleon case, the momentum flowing through the electron propagator cannot be much larger than $Q^2 \gg m_e^2$, otherwise the electron propagator strongly suppresses the integration. Therefore, the order of magnitude of $T(Q^2 \ll m_\mu^2) = \alpha g_{\phi\mu} / (6\pi^2 m_\mu)$ shows immediately that $F(K = 0) \sim \alpha^2 g_{\phi\mu} m_e / m_\mu$. Thus, compared with the nucleon coupling, the coupling to electrons is parametrically suppressed by the small ratio $m_e / m_\mu \sim 0.01$. We therefore neglect the effective coupling to electrons.

For vector bosons, the triangle diagram vanishes due

to charge conjugation invariance. The direct kinetic mixing between the vector boson and the photon does not produce fifth forces on neutral bodies, since the proton and the electron couple with opposite charges. More generally, higher-order diagrams with multiple photon insertions must respect electromagnetic gauge invariance. As a result, in the soft limit they cannot generate an unsuppressed coupling to the charge monopole of a neutral body: the electromagnetic current vanishes at zero momentum transfer, and the remaining gauge-invariant response is encoded in operators suppressed by powers of the exchanged momentum. Therefore, no long-range monopole fifth force is induced.